Molecular hyperfine interactions in Ag(CO)3

Ramiro ArratiaPerez and Dennis S. Marynick

Citation: The Journal of Chemical Physics **87**, 4644 (1987); doi: 10.1063/1.452827
View online: http://dx.doi.org/10.1063/1.452827
View Table of Contents: http://scitation.aip.org/content/aip/journal/jcp/87/8?ver=pdfcov
Published by the AIP Publishing

Molecular hyperfine interactions in $Ag(CO)_3$

Ramiro Arratia-Perez and Dennis S. Marynick
Deaprtment of Chemistry, University of Texas at Arlington, Arlington, Texas 76019-0065

(Received 24 February 1987; accepted 14 July 1987)

Relativistic molecular orbital calculations in the multiple scattering approximation are reported for silver tricarbonyl, and comparisons are made to optical absorption and electron spin resonance spectra. Spin–orbit effects are modelled through the Dirac scattered-wave (DSW) formalism. Spin–polarization effects are estimated from quasirelativistic spin-unrestricted calculations. The influence of different local density potentials on the spin distributions and hyperfine tensors are examined. The calculations show good agreement with optical spectral data and with the observed ^{107}Ag and ^{13}C hyperfine tensors. The use of relativistic exchange–correlation potentials in calculating spin-dependent properties leads to a slightly better agreement with experiment. The calculations predict that the unpaired electron in $Ag(CO)_3$ has about 40% silver $5p_z$ character.

I. INTRODUCTION

The carbonyls of copper, silver, and gold have attracted considerable attention because of their possible relevance to the mechanisms of carbon monoxide chemisorption on noble metals. Recently, with the utilization of matrix-isolation techniques at cryogenic temperatures, it has been possible to generate radicals of group 11 elements, and their vibrational, optical and electron spin-resonance spectra have been obtained and analyzed.[1–6] These studies showed that the tricarbonyls of Cu and Ag are bona fide complexes, while $Au(CO)_3$ is not formed. The paramagnetic complex $Ag(CO)_3$ has been synthesized in Ar, Kr, and Xe matrices from the cocondensation reaction of silver vapor and carbon monoxide at cryogenic temperatures.[1,3,5] The UV–visible and the ESR spectra in Ar matrices are consistent with a trigonal planar molecule having a $^2A_2''$ electronic ground state.[3,5,6] On the other hand, the ESR spectrum in adamantane matrices seems to be consistent with a pyramidal (C_{3v}) structure.[4] The existence of two conformers of $Ag(CO)_3$ may be rationalized in terms of matrix effects.[4–6] However, a geometry optimization via nonrelativistic *ab initio* SCF molecular orbital calculations[7] predicts the trigonal planar (D_{3h}) structure to be of lowest energy.

It is well recognized that the bonding scheme in silver tricarbonyl involves the participation of metal p and d orbitals through π back-donation to the ligands and ligand σ donation to empty metal orbitals.[7,8] *Ab initio* SCF[7] and nonrelativistic scattered-wave[8] studies disagree on the location of the unpaired electron. The *ab initio* calculation predicts that the unpaired spin is predominantly (54%) metal $5p_z$, while the scattered-wave calculation assigned the odd electron largely to the ligands. From the empirical analysis of the silver hyperfine tensors by Kasai and Jones[6] it was deduced that the unpaired electron has 53% $5p_z$ character. This is usually obtained by decomposing the observed coupling tensors into isotropic, anisotropic and orbital parts. The orbital contributions, which arise from spin–orbit coupling, have been neglected in many cases.[1,4–6] However, in first row transition metal complexes, it has been found that spin–orbit effects may contribute to the metal and ligand hyperfine interactions.[9,10] Moreover, it is risky to attempt to derive spin populations from the empirical estimate of the anisotropic portions of the hyperfine tensors of neutral complexes involving group 11 elements, because of their dependence upon $\langle r^{-3}\rangle_{np}$. In particular, both the spin–dipolar and orbi- contributions are expected to be approximately proportional to $\langle r^{-3}\rangle$ for the silver $5p$ orbital. Empirical analyses generally use atomic values for this,[4,6] whereas in the multiple scattering procedure this is determined by numerical integration of the radial Dirac equation in each molecular orbital. It has been shown earlier that molecular $\langle r^{-3}\rangle$ values differ from atomic values, since these orbitals are modified due to bond formation.[14] In fact, several conflicting $\langle r^{-3}\rangle_{np}$ values have been cited in the recent literature.[4,6,11–13]

In the present study we examine the role of different exchange–correlation potentials on molecular hyperfine interactions. We have used both Slater's original nonrelativistic statistical approximation[15] and the Hedin–Lundqvist potential[16] modified to include relativistic effects.[17,18] Our calculations using the relativistic exchange–correlation potential yields hyperfine tensors for both ^{107}Ag and ^{13}C that are in slightly better agreement with the observed values.

II. METHODS OF CALCULATION

The self-consistent-field Dirac scattered-wave (DSW) molecular orbital method is the relativistic extension of the nonrelativistic scattered-wave technique originally developed by Johnson.[19] The DSW methodology was first developed by Yang and Rabii[20] for calculations of bound-state wave functions, and has been recently reviewed.[21–23] This method uses the Dirac equation rather than the Schrödinger equation to generate the one-electron orbitals. Relativistic effects such as spin–orbit interaction, Darwin, and mass-velocity corrections are implicitly included at the SCF stage. Basically, the DSW method incorporates two fundamental assumptions. First, the wave function is approximated as a Slater determinant of four-component molecular spinors determined by an effective Coulomb and exchange–correlation potential; and second, the potential is spherically averaged inside cells surrounding each atomic nucleus, and outside an outer sphere that surrounds the entire molecule. The orbital energies are determined by solving the DSW secular equa-

 0021-9606/87/204644-07$02.10

tions and the resulting molecular orbitals, as well as the overall wave function, transform according to the extra irreducible representations of the molecular double point group under study.

For the exchange–correlation potential, we have used the original Slater $X\alpha$ potential in which the exchange α parameter is an adjustable one, usually determined by requiring the $X\alpha$ statistical energy to be the same as the Hartree–Fock total energy for atoms,[15] and the Hedin–Lundqvist (HL) potential[16] modified to include relativistic effects.[17,18] The HL function is similar to the Slater potential, but with a density-dependent α in which the contribution to the exchange and correlation energy at each point is assumed to be the same as that in a homogeneous electron gas of the same density. Thus, the HL potential adds Coulomb correlations not included in the simplest $X\alpha$ potential.[16] The relativistic exchange–correlation potentials have been tested in atomic calculations. These exhibit important differences from their nonrelativistic counterparts in regions of high electron density, but are very similar in the low electron density regions characteristic of valence orbitals of the atoms.[24] Here we present the first relativistic molecular calculations using relativistic local potentials in calculating spin–dependent properties.[21]

We also performed quasirelativistic scattered-wave calculations using the method of Koelling and Harmon.[25] These calculations incorporate the Darwin and mass-velocity corrections, but leave out the spin–orbit term. Because spin is still a good quantum number, one can perform spin-unrestricted calculations in the usual manner, giving a qualitative picture of the effects of core spin–polarization. Thus, the spin–up and spin–down orbitals are distinct, so that in general the resulting wave function (which transforms according to the single point group) is not a spin eigenfunction.

A quantitative structural determination of $Ag(CO)_3$ by routine physical methods has not been performed, due to the inability to experiment with this radical outside of a frozen gas matrix. We have chosen the Ag–C bond length equal to 2.11 Å (in calculations A and B), which is equal to the sum of the covalent radii of the atoms,[8] and equal to 2.32 Å (in calculations C and D) which was obtained by an *ab initio* SCF nonrelativistic calculation.[7] The C–O bond length was set equal to 1.16 Å in all the calculations. The multiple scattering parameters used in the calculations are given in Table I. A minimum basis of angular functions was used, with l through 4 on the outer sphere, l through 2 on Ag, and l through 1 on C and O. The basis functions for the D_{3h} double group were generated according to Yang's symmetrization procedure.[26] In our notation the extra irreducible representations are related to Bethe's notation as follows: $e_1 \leftrightarrow \gamma_7$, $e_2 \leftrightarrow \gamma_8$, and $e_3 \leftrightarrow \gamma_9$.

The method used for the calculation of the hyperfine interactions has been described elsewhere,[9,10,27–32] and is based upon a first-order perturbation to the Dirac Hamiltonian so that the effects of external magnetic fields are described by the perturbation operator $\mathscr{H}'$, where

$$\mathscr{H}' = e\boldsymbol{\alpha}\cdot\mathbf{A}. \tag{1}$$

In Eq. (1) $\boldsymbol{\alpha}$ is the vector of 4×4 Dirac matrices and $\mathbf{A}$ is the electromagnetic vector potential. For the hyperfine term $\mathbf{A} = (\boldsymbol{\mu}\times\mathbf{r})/r^3$, where $\boldsymbol{\mu}$ is the nuclear magnetic moment. Matrix elements of these operators are evaluated for the two rows of the e_2 representation of the highest occupied molecular orbital. The resulting perturbation energies are then fitted to the usual spin-Hamiltonian for hyperfine interactions,

$$\mathscr{H}_{\text{spin}} = \mathbf{S}\cdot\mathbf{A}_n\cdot\mathbf{I}_n. \tag{2}$$

In Eq. (2), a value of $\mathbf{S} = 1/2$ is used to decribe the ground state Kramers doublet, $\mathbf{I}_n$ is the nuclear spin operators, $\mathbf{A}_n$ is the hyperfine coupling tensor, and n = Ag, C, or O.

TABLE I. Parameters used in the calculations.[a]

	A, B	C, D
Ag–C bond length	2.11[b]	2.32[c]
C–O bond length	1.16	1.16
Sphere radii:		
Ag	1.35	1.46
C	0.87	0.88
O	0.87	0.87
Out	4.03	4.25

[a] All values in Å.
[b] Reference 8.
[c] Reference 7.

III. RESULTS AND DISCUSSION

A. Orbital energies

Figure 1 shows the upper valence orbital energies for four Dirac scattered-wave (DSW) calculations on $Ag(CO)_3$. Columns A, B and C, D report calculations performed at d(Ag–C) = 2.11 and 2.32 Å, repsectively.[7,8] Columns A and C give results of DSW calculations using the nonrelativistic $X\alpha$ Slater potential, whereas columns B and D give results of the DSW calculations using the relativistic exchange–correlation potentials described above. For all the calculations, the upper valence electronic structure is divided into: (a) the unoccupied band which is comprised of CO $2\pi^*$ and Ag–C σ^* orbitals, (b) the partially occupied $7e_2$ MO, (c) the occupied silver $4d$ crystal field-like orbitals (the d band), and (d) the $\sigma + \pi$ (or ligand) band which is comprised largely of 5σ and 1π CO orbitals with some metallic character. By comparing column A against column B we observe that the general valence structure is nearly the same, except for a rigid shift downward by about 0.4 eV. The same situation is seen in columns C and D. The spacings and spin–orbit splitting of the energy levels are nearly the same in all the calculations. The spin–orbit splittings of the de' (into $6e_2$ and $7e_3$) and the de'' (into $6e_3$ and $6e_1$) molecular orbitals are about 0.25 and 0.30 eV, respectively. These calculated values could be useful if the photoelectron spectrum of silver tricarbonyl is measured in the near future, and are very similar to the observed[33] and calculated[34] spin–orbit splitting (0.26 eV) of the $5d(t_{2g})$ orbitals in $W(CO)_6$. Moreover, the splittings in $Ag(CO)_3$ are larger than in $Cu(CO)_3$, where the metal based $3d$ orbitals split by $\sim$0.15 eV.[10] This is ex-

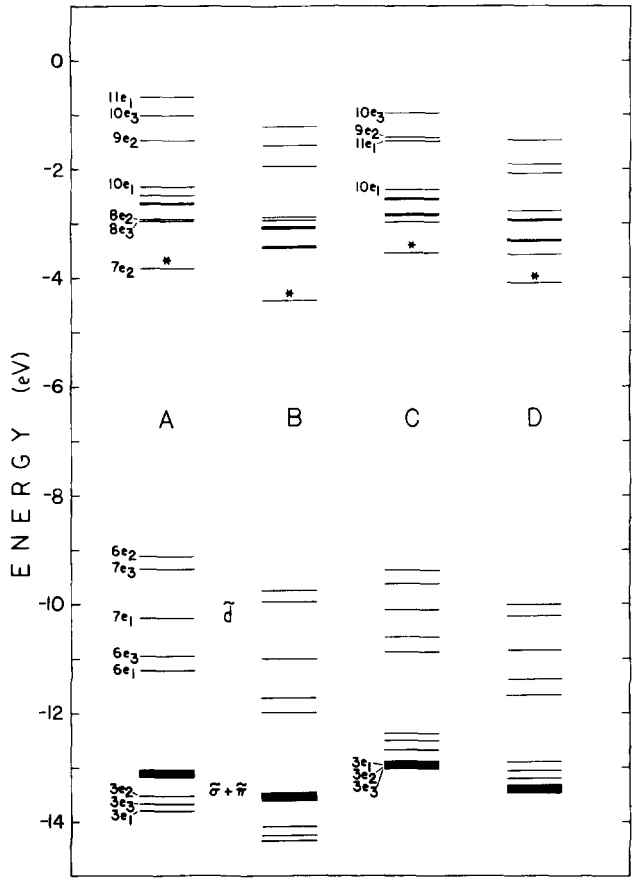

FIG. 1. Orbital energies for four DSW calculations on $Ag(CO)_3$. Calculations A and B were performed at $d(Ag–C) = 2.11$ Å, and calculations C and D were performed at 2.32 Å. Calculations A and C used the $X\alpha$ potentials. Calculations B and D used the relativistic exchange–correlation potentials; see the text. The highest occupied orbital is marked with an asterisk.

pected since relativistic effects are larger in Ag than Cu. The calculated d bandwidth of $Ag(CO)_3$ in calculations A, B, C, and D amounts to 2.1, 2.2, 1.6, and 1.8 eV, respectively. In copper tricarbonyl, the corresponding value is only 1.3 eV.[10] The widths of the ligand band in calculations A, B, C, and D are 0.8, 0.9, 0.6, and 0.5 eV, respectively. In copper tricarbonyl, the ligand band is larger and amounts to 1.2 eV. The energy gap between the HOMO ($7e_2$) and the top of the d band in silver tricarbonyl is 5.3 eV (calculations A and B) and 5.8 eV (calculations C and D), while in copper tricarbonyl it is 4.3 eV. This energy gap difference is associated with the observed red shift of one of the absorption bands of $Ag(CO)_3$ with respect to $Cu(CO)_3$,[2,3,8] as discussed below.

The change of Ag–C bond length from 2.11 (A and B) to 2.32 Å (C and D) induces some reordering of energy levels in the unoccupied and ligand bands, as indicated in Fig. 1. For example, the bottom of the ligand band ($3e_2$, $3e_3$, and $3e_1$) in calculations A and B corresponds to MOs which contain about 38% metal character. The equivalent MOs in calculations C and D are located at the top of the ligand band. As in $Cu(CO)_3$, the orbitals located in the ligand band are significantly spin–orbit contaminated (i.e., the minority spin present in the relativistic MOs amounts to about 25%)[10] due to their close proximity, while the metal based $4d$ orbitals ($6e_1$ and $7e_1$) are spin–orbit contaminated by only 5%. The bonding mechanism of $Ag(CO)_3$ is similar to $Cu(CO)_3$, which was discussed in detail previously,[10] and need not be repeated here. The analysis of the valence charge distribution in $Ag(CO)_3$ (calculation A) indicates that ligand donation to Ag amounts to 1.22 electrons (0.594 to $5s$ and 0.626 electrons to $5p$), whereas backdonation (Ag→CO) amounts to 0.86 electrons (0.70 through $5p_z$ and 0.16 through $4d$). This indicates that there is a net charge transfer of 0.12 electrons per carbonyl from the ligand to the metal which is exactly the same as in $Cu(CO)_3$. A similar situation was observed in the hexacarbonyls of Cr, Mo, and W, where the charge transfer invariably amounts to 0.46 electrons from ligand to metal.[34]

B. Transition state calculations

The ultraviolet–visible spectra of $Ag(CO)_3$ recorded in a pure CO matrix consists of two very intense, broad absorptions centered at about 680 and 457 nm, and weak shoulders at 580, 420, and 225 nm.[3,5,8] A crude assignment of the electronic transitions was made by McIntosh *et al.*[8] by taking the ground state energy differences (i.e., not allowing for electronic relaxation upon electron excitations). Their results were within a factor of 2 of the observed quantities (for example, McIntosh *et al.* predicted the lowest excitation at 1110 nm while the observed band is centered at about 680 nm). Morover, their assignment for the lowest transition is from the HOMO to the mainly $2\pi^*$ ligand MO ($3e''$),[8] whereas our assignment involves the HOMO and the Ag–C σ^* ($10e_1$) orbitals. A transition state calculation is required because the electronic excitations involves the HOMO orbital whose energy should be quite sensitive to the significant metal character. It is well known that the use of Slater's transition state (TS) method is a convenient approach within the local density theory to estimate relaxation corrections to excitation energies.[15,19,21] In principle, the highest accuracy is obtained by doing separate TS calculations (until SCF convergence is reached) for every transition of interest. In the present study we have performed DSW-TS calculations (A) to estimate the first ionization potential (IP) and excitation energies of $Ag(CO)_3$. The predicted and observed energies for the lowest dipole allowed excitations in $Ag(CO)_3$ along with those corresponding to copper tricarbonyl[10] are presented in Table II. The predicted values are in good agreement with the experiment.[2,3,8] The two intense bands and the weak shoulder ($7e_2 \rightarrow 11e_1$) are assigned to ligand–ligand electronic transitions, while the excitation from a highly localized metal d orbital ($7e_3$) to the HOMO is assigned as metal–ligand charge transfer (MLCT). It is of interest to compare the predicted electronic transitions of $Ag(CO)_3$ and $Cu(CO)_3$ with those observed experimentally (see Table II). The predicted transitions of silver tricarbonyl are shifted to lower energies compared to the corresponding ones of copper tricarbonyl. The same trend is seen experimentally.[2,3,8] Our symmetry analysis indicates that the weak absorption band seen at 580 nm could be attributed to matrix effects, in accord with the experimental suggestion for the corresponding band in the copper complex (at 495 nm).[2] We have also calculated the first IP for $Ag(CO)_3$ which is

TABLE II. Excitation energies.[a]

Transition	Calculated[b]	Observed[c]
$7e_2 \rightarrow 10e_1$	760 (607)[d]	680 (562)
$7e_2 \rightarrow 10e_3$	430 (368)[d]	457 (375)
$7e_2 \rightarrow 11e_1$	384 (318)[d]	420 (344)
$7e_3 \rightarrow 7e_2$	198 (230)[d]	225 (262)

[a] All units in nm. Values in parentheses are for $Cu(CO)_3$.
[b] Obtained according to the DSW-TS-$X\alpha$ calculations.
[c] References 1–3, 5, and 8.
[d] Reference 10.

predicted to be 6.2 eV, smaller than the calculated IP for $Cu(CO)_3$ at 6.6 eV.[10]

C. Spin distributions and hyperfine interactions

In the present DSW spin-restricted calculations, all the spin density arises from the highest occupied orbital. Table III gives the populations for the partially occupied orbital ($7e_2$) from the quasirelativistic spin-unrestricted and the four DSW calculations. The DSW orbital characters are reported in terms of a Pauli description consisting of spherical harmonics multiplied by spin functions. In this charge decomposition procedure we consider only the two large components of the relativistic wave function, and assume that the radial wave functions inside each atomic sphere are the same for $l = j - 1/2$ and $l = j + 1/2$. The sum of two such spinors can then be interpreted as a nonrelativistic function of mixed spin, with spin α corresponding to column 1 and spin β to column 2. The HOMO level is virtually unaffected by spin–orbit mixing since the ratio of spin–down to spin–up character is less than 10^{-3}. However, this small amount of minority spin mixed into the HOMO will introduce small orbital contributions to the hyperfine interactions, as discussed below. As shown in Table III, all the calculations predict that most of the unpaired electron density (spin–up) is distributed among the ligands. It is also seen that the calculations using the relativistic exchange–correlation potentials (B and D) predict larger populations (by $\sim 5\%$) on the silver atom, than those using the $X\alpha$ potentials (A and C).

TABLE III. Spin populations.[a]

Method	Spin	Ag (5p)	C (2p)	O (2p)
QRU[b]	α	0.316	0.161	0.067
DSW-A[c]	α	0.295	0.175	0.060
DSW-B[d]	α	0.345	0.161	0.057
DSW-C[c]	α	0.343	0.168	0.051
DSW-D[d]	α	0.403	0.158	0.048
SCF-HF[e]	α	0.540	0.010	0.050
Emp.[f]		0.530	0.084	0.080

[a] Charge breakdown of DSW calculations is in terms of Pauli decomposition, see the text.
[b] QRU, quasirelativistic spin-unrestricted calculation.
[c] DSW calculations using the $X\alpha$ potentials.
[d] DSW calculations using the relativistic exchange–correlation potentials of Refs. 16–18.
[e] Nonrelativistic *ab initio* SCF calculation, Ref. 7.
[f] Empirical analyses, Ref. 6.

This small change in metal populations will be reflected in the silver hyperfine tensors. The total metal 5p population is predicted to be 35% (calculation B) and 40% (calculation D), respectively. These values are somewhat smaller than those estimated (53%) from the observed silver hyperfine tensors.[6] It should be noted, however, that the silver population was empirically deduced by scaling the anisotropic part of the molecular hyperfine tensor to the corresponding values (52 MHz) for the silver atom, in which the $\langle r^{-3} \rangle_{5p}$ value was estimated from the hyperfine splitting term of the ^{115}In atom.[6] Obviously, this choice of $\langle r^{-3} \rangle$ is unrealistic. It has been shown earlier[27–29] that atomic $\langle r^{-3} \rangle$ values differ significantly from the corresponding molecular values. Several points concerning the empirical estimate of 53% 5p character deserve comment: (a) Kasai and Jones,[6] by using the usual decomposition procedure of the total silver hyperfine tensors into isotropic and anisotropic parts (which are not directly determined from the ESR experiment), obtained a value of 28 MHz for the spin–dipolar (anisotropic) interactions. It is has been recently demonstrated that this decomposition procedure is not suitable when analyzing ESR data for transition metal complexes since spin–orbit effects may contribute to the metal and ligand hyperfine interactions.[9,10,27–32] Our relativistic calculation (B), which includes spin–orbit effects, predicts the silver anisotropic interaction to be equal to 20 MHz, which is slightly smaller than the empirical estimate. (b) The empirical estimate for the spin–dipolar interaction (28 MHz) was scaled against the atomic value of 52 MHz. Since the dipolar interaction for p orbitals can be related to $\langle r^{-3} \rangle$ as $A_{\text{dip}} = (2/5) g_e g_N \beta_N \beta_e \langle r^{-3} \rangle_p$, for a unit spin density,[6,35] the empirical estimate of Kasai and Jones[6] of 53% 5p metal character corresponds to $\langle r^{-3} \rangle = 5.9882$ a.u.$^{-3}$. We have calculated $\langle r^{-3} \rangle$ for the silver 5p orbital in $Ag(CO)_3$ and find it to be equal to 5.2965 a.u.$^{-3}$. Our calculated value indicates that the silver orbital is significantly more expanded in the molecule. (c) We have also calculated the effects of spin–orbit coupling in the silver hyperfine interactions, i.e., the extent of the "orbital" contributions that arise from unquenched orbital angular momentum. Our calculations reveal that the orbital contributions to the total parallel silver hyperfine tensor amount to 5 MHz, whereas the contributions to the perpendicular component amount to -8 MHz. These small orbital contributions are consistent with the small deviations of the observed g tensors from the spin-only (g_e) value.[6] These values indicate that the empirical estimate of the silver dipolar interaction may be overestimated and consequently so is the amount of 5p metal character, since the experimental analysis did not include spin–orbit effects and used unmodified $\langle r^{-3} \rangle$ atomic values. If the empirical estimate of 28 MHz is corrected by a small amount of orbital contribution (by ~ 5 MHz) we obtain an estimate of $\sim 45\%$ 5p metal character, which is in better agreement with our value of $\sim 40\%$. We can also compare our calculated spin population with the *ab initio* calculated[7] value of 54%, keeping in mind possible differences between Mulliken populations based on LCAO theories and the present partial wave analysis. The difference between the two estimates may be more apparent than real. A major portion of this discrep-

ancy undoubtedly lies in the fact that the silver $5p$ orbital of LCAO theories extends to infinity, while the partial wave in the multiple scattering description is confined to the finite cellular region about the silver nucleus. Nevertheless, the fact that we are able to reproduce the silver hyperfine tensors (see below) with a 40% spin population on silver suggests that our analysis is meaningful.

Let us now consider the analysis of the total ^{107}Ag hyperfine tensors. The calculated and experimental results are given in Table IV. The calculated DSW values demonstrate that the silver hyperfine tensors are anisotropic, but the DSW values are far from the experimental results. All of the DSW values come from the one-center, spin–dipolar interaction and orbital term, since the Fermi contact contributions vanish by symmetry. It is plausible to ascribe much of the difference between the DSW and experimental results to core polarization effects not present in the spin-restricted DSW wave function. To estimate such effects, we have carried out spin-unrestricted quasirelativistic calculations using the $X\alpha$ potential and setting $d(\text{Ag–C}) = 2.11$ Å and have calculated the spin density at the Ag nucleus for such a wave function. The result is $-0.115\,a_0^{-3}$, which corresponds to a Fermi contact contribution of 20.8 MHz (since the ^{107}Ag g-nuclear factor is equal to -0.227). This calculated value is in very close agreement with the empirical value of 23 MHz.[6] We have also estimated from the quasirelativistic spin-unrestricted wave function a small two-center, spin–dipolar interaction arising from the spin at the CO site. By adding up the DSW values plus those quantities estimated from the spin-unrestricted wave function we obtained good agreement between theory and experiment (see Table IV). The same approach has yielded good agreement with observed hyperfine tensors in Cu and Np complexes.[9,10,30] More elaborate methods of including spin–polarization effects in four component theories have been proposed.[36,37] The relativistic determination of core spin–polarization hyperfine interactions in atomic systems has been pursued via Dirac–Fock (DF) theory.[36] Here, the radial core polarization of the one-electron atomic spinors is obtained by relaxing the constraint of restricted DF theory that the large and small components of the radial part be independent of the magnetic quantum number.[36] Also, the relativistic generalization of the Bloch theory of a magnetic electron gas has been developed by Ramana and Rajagopal,[37] in which the projection operators for states of positive energy and given spin were deduced for the relativistic spin–polarized electron gas.[37] To our knowledge no relativistic spin–polarized molecular calculations have been yet reported, although approximate methods of including spin-polarization effects via scalar relativistic spin-unrestricted calculations have been discussed.[29,30]

Our calculations show the silver hyperfine tensors to be axially symmetric, while the experiment apparently shows slight deviation (-1.4 MHz) from axial symmetry.[6] Our results strongly suggest that this slight deviation could be attributed to matrix effects. From Table IV it is seen that closer agreement with experiment is obtained from those calculations (B and D) that utilize the relativistic exchange–correlation potentials, but the differences are not quantitatively significant. The difference between the two types of local potentials could be ascribed in part to relativistic effects and in part to the effects of electron correlation, which is treated differently in the Hedin–Lundqvist function.[38] Relativistic local potentials will probably be more effective in calculating spin-dependent properties in systems containing heavier atoms.

Table V gives the calculated and experimental results for ^{13}C hyperfine interactions. It can be seen that the DSW results do not compare well with experiment. Again, much of the difference between the DSW and experimental results can be ascribed to core–polarization effects. The Fermi con-

TABLE IV. ^{107}Ag hyperfine interactions.[a]

	$A_{\parallel}$	$A_{\perp}$
DSW result A[b]	35.4	−22.6
DSW result B[b]	38.8	−24.7
DSW result C[c]	34.8	−24.1
DSW result D[c]	39.1	−26.9
Core spin–polarization[d]	20.8	20.8
Spin–dipole coupling[e]	5.6	−2.8
Total A	61.8	−4.6
Total B	65.2	−6.7
Total C	61.2	−6.1
Total D	65.5	−8.9
Experiment[f]	78.0	−7.8

[a] All units in MHz. Calculations A and C use the $X\alpha$ potentials. Calculations B and D use the relativistic exchange–correlation potentials.
[b] Calculated at $d(\text{Ag–C}) = 2.11$ Å.
[c] Calculated at $d(\text{Ag–C}) = 2.32$ Å.
[d] Calculated from the QRU calculation.
[e] Interaction between the electron spin on the CO ligand with the ^{107}Ag nucleus as obtained from the QRU calculation.
[f] Reference 6.

TABLE V. ^{13}C and ^{17}O hyperfine interactions.[a]

	A_{xx}	A_{yy}	A_{zz}
^{13}C			
DSW result A	−18.6	−17.4	29.3
DSW result B	−15.6	−14.8	24.6
DSW result C	−19.5	−17.1	28.2
DSW result D	−15.9	−14.1	23.1
Core spin–polarization[b]	−21.5	−21.5	−21.5
Total A	−40.1	−38.9	7.8
Total B	−37.1	−36.3	3.1
Total C	−41.0	−38.6	6.7
Total D	−37.4	−35.6	1.6
Experiment[c]	−24.0	−24.0	3.0
^{17}O			
DSW result A	14.5	13.6	−24.1
DSW result B	13.1	12.4	−21.9
DSW result C	14.2	12.4	−21.7
DSW result D	12.5	11.0	−19.2
Core spin–polarization[b]	2.1	2.1	2.1
Total A	16.6	15.7	−22.0
Total B	15.2	14.5	−19.8
Total C	16.3	14.5	−19.6
Total D	14.6	13.1	−17.1

[a] All units in MHz.
[b] Obtained from the QRU calculation.
[c] The XX component was approximated to be equal to the YY component, see Ref. 6.

tact interaction, which arises due to spin–orbit mixings into the HOMO, is allowed by symmetry in the DSW calculations but it is very small (-0.2 MHz). The carbon Fermi term vanishes by symmetry in the nonrelativistic limit. In order to estimate these effects, we have calculated the spin density at the carbon nucleus by using the spin-unrestricted wave function. The result is $-0.019\ a_0^{-3}$, which corresponds to a Fermi contact contribution of -21.5 MHz, in reasonable agreement with the empirical value of -15 MHz.[6] Our calculations predict some rhombic character (~ 1.2 MHz) in the ^{13}C hyperfine tensors. This effect is probably due to contributions to the partially occupied state from the $2p_{3/2}$ spinors. This suggests some degree of magnetic inequivalency between the carbon nuclei, since the hyperfine tensors reflect the symmetry of the electronic distribution at this site, which is not necessarily the point-group symmetry of the complex. In fact, Kasai and Jones[6] approximated the XX components to be equal to the YY components. It is also interesting to note some extra broadening of the peaks in the ESR spectra which can be attributed to a small departure of the ^{13}C hyperfine tensors from axial symmetry.[6] The same situation was observed in copper tricarbonyl.[10] The agreement between theory and experiment is quite satisfactory and the use of relativistic exchange–correlation potentials leads to a slightly better agreement with experiment (see Table V). To estimate the effects of spin–orbit interaction on the carbon hyperfine tensors, we have made an approximate decomposition of the total hyperfine tensors into Fermi, spin–dipolar, and orbital terms, as has been done previously.[9,10,27–32] Our results indicate that the orbital contributions to the C hyperfine tensors amount to -2.6, 0.2, and -3.4 MHz for the XX, YY, and ZZ components, respectively. It is worth noting that, even though carbon is a light atom, the orbital contributions to its hyperfine tensors are not negligible. This interaction arises from unquenched orbital angular momentum which is neither isotropic nor traceless, so that the experimental decomposition of the total hyperfine tensors into isotropic and anisotropic parts has little utility when a light atom is bound to a heavier atom. Recent fully relativistic studies of F bound to Xe[27] or Np,[30] for N in copper phorphyrin[9] and for C and O in copper tricarbonyl[10] reached the same conclusions.

The predicted hyperfine tensors of ^{17}O are also given in Table V. These may be of some use in interpreting spectra if the ESR spectrum of enriched oxygen samples is ever investigated. It is seen that core spin–polarization contributions are rather small (2.1 MHz). Our calculations also predict a small axial departure (1–2 MHz) of the hyperfine tensors. We have also estimated the contributions from orbital motions. These are not negligible and amount to -0.9, 0.6, and 3.7 MHz, for the XX, YY, and ZZ components, respectively. Thus, spin–orbit effects introduce small amounts of orbital contributions at the oxygen and carbon sites. These effects should be taken into account when attempting to derive bonding information from the ESR parameters.

IV. CONCLUSIONS

In this paper we have tried to obtain a detailed interpretation of the available experimental data on silver tricarbonyl. The calculated electronic transitions satisfactorily account for the UV–visible bands seen in the optical spectra. Spin–polarization effects have a large contribution to the ^{107}Ag and ^{13}C hyperfine tensors, since the Fermi contact interaction is a significant portion of the total hyperfine interactions. Spin–orbit effects introduce small orbital contributions to the hyperfine tensors at the Ag, C, and O sites. We have also shown that the use of atomic $\langle r^{-3}\rangle_{5p}$ values and the neglect of orbital motions may lead to an overestimate of the metal $5p$ spin populations. Our calculations also found that there is a small axial departure of the carbon and oxygen hyperfine tensors. The calculations of spin-dependent properties using relativistic exchange–correlation potentials differ from those using the $X\alpha$ potentials by about 10% and lead to a slightly better agreement with experiment, although qualitatively unimportant. Due to the spin-restricted nature of the DSW wave function, it is necessary to estimate spin–polarization effects from spin–unrestricted scalar relativistic wave functions. In general, the agreement between theory and experiment is quite satisfactory.

ACKNOWLEDGMENTS

We thank David Case for encouragement and advice. This work was supported in part by grants from the Robert A. Welch Foundation (Grant No. Y-743) and Cray Research Inc.

[1] M. Moskovitz and G. A. Ozin, in *Cryochemistry* (Wiley–Interscience, New York, 1975).
[2] H. Huber, E. P. Kundig, M. Moskovitz, and G. A. Ozin, J. Am. Chem. Soc. **97**, 2097 (1975).
[3] G. A. Ozin, App. Spectrosc. **30**, 573 (1976).
[4] J. A. Howard, B. Mile, J. R. Morton, and K. F. Preston, J. Phys. Chem. **90**, 2027 (1986).
[5] D. F. McIntosh and G. A. Ozin, J. Am. Chem. Soc. **98**, 3167 (1976).
[6] P. H. Kasai and P. M. Jones, J. Phys. Chem. **89**, 1147 (1985); J. Am. Chem. Soc. **107**, 813 (1985).
[7] J. T. Tse, Ber. Bunsenges. Phys. Chem. **90**, 906 (1986).
[8] D. F. McIntosh, G. A. Ozin, and R. P. Messmer, Inorg. Chem. **20**, 3640 (1981).
[9] D. A. Case, in *Porphyrins. Excited States and Dynamics*, edited by M. Gouterman, P. M. Reutzepis, and K. I. Straub, Am. Chem. Soc. Symp. Ser. 321 (American Chemical Society, Washington D.C., 1986), p. 59.
[10] R. Arratia-Perez, F. U. Axe, and D. S. Marynick, J. Phys. Chem. (in press).
[11] J. A. Howard, B. Mile, J. R. Morton, K. F. Preston, and R. J. Sutcliffe, J. Phys. Chem. **90**, 1033 (1986).
[12] A. J. Buck, B. Mile, and J. A. Howard, J. Am. Chem. Soc. **105**, 3381 (1983).
[13] D. M. Lindsay and P. H. Kasai, J. Magn. Reson. **64**, 278 (1985).
[14] D. A. Case and M. Karplus, J. Am. Chem. Soc. **99**, 6182 (1977).
[15] J. C. Slater, *Quantum Theory of Molecules and Solids* (McGraw–Hill, New York, 1974), Vol. IV.
[16] L. Hedin and B. I. Lundqvist, J. Phys. C **4**, 2064 (1971).
[17] A. H. McDonald and S. H. Vosko, J. Phys. C **12**, 2977 (1979).
[18] A. K. Rajagopal, J. Phys. C **11**, L943 (1978).
[19] K. H. Johnson, Adv. Quantum Chem. **7**, 143 (1973).
[20] C. Y. Yang and S. Rabii, Phys. Rev. A **12**, 362 (1975).
[21] D. A. Case, Annu. Rev. Phys. Chem. **33**, 151 (1982).
[22] C. Y. Yang, in *Relativistic Effects in Atoms, Molecules and Solids*, edited by G. L. Malli (Plenum, New York, 1983), p. 335.
[23] C. Y. Yang and D. A. Case, in *Local Density Approximations in Quantum Chemistry and Solid State Physics*, edited by J. P. Dahl and J. Avery (Plenum, New York, 1984), p. 643.
[24] M. P. Das, M. V. Ramana, and A. K. Rajagopal, Phys. Rev. A **22**, 9 (1980).
[25] D. D. Koelling and B. N. Harmon, J. Phys. C **10**, 3107 (1977).

[26]C. Y. Yang, J. Chem. Phys. **68**, 2626 (1978).
[27]R. Arratia-Perez and D. A. Case, J. Chem. Phys. **79**, 4939 (1983).
[28]D. A. Case and J. P. Lopez, J. Chem. Phys. **80**, 3270 (1984).
[29]J. P. Lopez and D. A. Case, J. Chem. Phys. **81**, 4554 (1984).
[30]D. A. Case, J. Chem. Phys. **83**, 5792 (1985).
[31]R. Arratia-Perez and G. L. Malli, J. Chem. Phys. **84**, 5891 (1986).
[32]R. Arratia-Perez and G. L. Malli, J. Chem. Phys. **85**, 6610 (1986).
[33]J. L. Hubbard and D. L. Litchtenberger, J. Am. Chem. Soc. **104**, 2132 (1982).
[34]R. Arratia-Perez and C. Y. Yang, J. Chem. Phys. **83**, 4005 (1985); C. Y. Yang, R. Arratia-Perez, and J. P. Lopez, Chem. Phys. Lett. **107**, 112 (1984).
[35]J. R. Morton and K. F. Preston, J. Magn. Reson. **30**, 577 (1978).
[36]J. P. Desclaux, A. J. Freeman, and J. V. Mallow, J. Magn. & Magn. Mater. **5**, 265 (1977).
[37]M. V. Ramana and A. K. Rajagopal, J. Phys. C **12**, L845 (1979).
[38]See a recent article about electron–correlation and local density methods, M. Cook and M. Karplus, J. Phys. Chem. **91**, 31 (1987).